

Received October 6, 2021, accepted October 21, 2021, date of publication October 29, 2021, date of current version November 8, 2021.

Digital Object Identifier 10.1109/ACCESS.2021.3124205

# An Enhanced Algorithm for Conventional Protection Devices of Transmission Lines With DTLR

ELSAEED ALI<sup>1,2</sup>, (Member, IEEE), AND ANDREW M. KNIGHT<sup>1</sup>, (Senior Member, IEEE)

<sup>1</sup>Department of Electrical and Software Engineering, University of Calgary, Calgary, AB T2N 1N4, Canada

<sup>2</sup>Department of Electrical Engineering, Mansoura University, Mansoura 35516, Egypt

Corresponding author: Elsaeed Ali (elsaeed.ali@ucalgary.ca)

This work was supported in part by the Natural Sciences and Engineering Research Council (NSERC) of Canada, in part by Alberta Electric System Operator (AESO), in part by ATCO Electric, and in part by Altalink under Grant CRDPJ 500547.

**ABSTRACT** As the installed capacity of renewable generation continues to increase nowadays to satisfy both emissions and economic requirements, the nature of intermittent generation results in a need to further increase transmission capacity. Dynamic thermal line rating may be used to increase the capacity of transmission lines without upgrading infrastructure. However, existing transmission line protection devices may mal-operate due to the increased capacity. So, it is required to evaluate the performance of existing protection devices. This paper proposes an algorithm that enhances the performance of existing conventional relays such as distance and overcurrent relays. The proposed algorithm is based on a combination of dynamic thermal rating, current ratio of negative and positive sequences and voltage criterion to detect faults whether symmetrical or asymmetrical and unsafe overload. In addition, it aims at restraining the existing relays during safe overloads. A model of a system under investigation is simulated, with studies performed in a MATLAB/Simulink environment. The results demonstrate the ability of the proposed scheme to detect all types of faults and unsafe overload dependably and restrain the conventional relays securely during safe overloads.

**INDEX TERMS** Dynamic line rating, ampacity, transmission lines, distance protection, overcurrent protection, faults, overloads.

## I. INTRODUCTION

With the increasing demand of electrical power, power systems are becoming more complex. Thus, power system operators are facing many challenges due to that complexity. Fulfilling this demand requires a large increase of generation capacity. Consequently, the infrastructure of transmission system requires high-cost upgrading. Dynamic thermal line rating (DTLR) is considered one of the alternative solutions to increase the capacity of existing overhead transmission lines (TLs). The thermal rating of TL is basically determined for different seasons based on the worst weather conditions. This rating is kept constant for the entire season and called as static line rating (SLR). Unlike SLR, DTLR is based on real-time measurements of environmental conditions such as ambient temperature, wind speed and wind direction to update the rating. Transmission line ratings whether static or dynamic

are calculated based on the heat balance equation in IEEE Standards 738 [1]. During favorable weather conditions, the system operators can use the full benefits of TL by increasing its capacity according to DTLR calculations. Furthermore, using DTLR can reduce conductor sag and consequently prevent early aging of TL owing to increased conductor temperature.

It is reported that DTLR might increase the ampacity of TL located in windy areas up to 200% of SLR [2], [3]. Avoiding replacement of other elements in the system, the increased ampacity may be limited to 25% [4]. However, there is still significant concern in industry about the ability to integrate DTLR with overload protection with the existing conventional relays infrastructure. Thus, the amount of increased capacity may be seen by TL conventional relays as fault. So, the performance of existing protection devices could be affected and could mal-operate due to overloading from DTLR.

The associate editor coordinating the review of this manuscript and approving it for publication was Arturo Conde<sup>1</sup>.

The most common protection devices with TL are distance and overcurrent (OC) relays [5], [6]. Usually, OC is used as a back-up protection for distance relay [6], [7]. Therefore, it is required to evaluate TL conventional protections with DTLR. Several studies have been performed on detecting fault conditions such as pilot protection schemes [8]–[10], differential protection approaches [11], [12], travelling-wave-based methods [13]–[15], wavelet-based algorithms [16]–[18], and sequence components algorithms [19]–[22]. These approaches focused on discrimination between normal and fault conditions whether internal or external. Moreover, the overloading conditions have not been investigated and differentiated from fault conditions.

Studies reported in the literature for TL protection with DTLR are very limited [23]–[30]. A probabilistic overload protection scheme has been used in [23] and [24] to detect unsafe overload conditions based on the probability distribution of conductor temperature. During overload conditions between 1.2 – 1.5 of nominal current, the classical relays failed to detect 48% of unsafe overload cases, while a probabilistic scheme failed to detect 39% of these cases. Thus, the probabilistic scheme does not add a significant improvement and lacks dependability. DTLR algorithm has been proposed in the UK transmission system to enable a larger penetration of wind generation [25]–[27]. The algorithm is used as a back-up protection to the control system. The protection scheme sends a trip signal to isolate the wind farm after a time delay when the measured current is higher than a certain percentage of the permissible ampacity. However, there are no studies for unsafe overload cases which evaluate the performance of the protection algorithm. In [28] and [29], DTLR has been integrated into an existing operational tripping scheme to enhance its performance to reduce the unnecessary tripping of generation because of violating thermal rating of the line. Dynamic thermal rating has been used in [30] to enhance OC relay to detect symmetrical fault conditions and unsafe overload, and restrain the relay during safe overload and power swing. In [31], the same algorithm used in [30], has been augmented with distance relay to restrain the relay during overloading and power swing conditions in Zone 3. Both algorithms used the fact that the current value during fault conditions has a high dynamic compared to overloading conditions. Unlike overloading conditions, the rate of change of the current during fault conditions will be larger than a predefined limit. However, there is no information about detecting asymmetrical faults despite they are the most common faults compared to symmetrical faults [32]. In addition, the performance of the proposed algorithm during fault conditions, especially at the far-end of Zone 3, has not been evaluated. Indeed, if the fault condition, whether symmetrical or asymmetrical, has taken place at the far-end of Zone 3, the relay might mal-operate. In this case, the relay will not be able to differentiate between safe overloading and fault conditions.

In this paper, DTLR with the aid of current ratio of negative and positive sequences ( $I_-/I_+$ ), and voltage criterion are

augmented with the existing conventional protection devices, namely distance and overcurrent relays to enhance their performance during fault and overload conditions. This paper represents the mathematical equations of DTLR in Section II and the basic principles of distance protection and overcurrent relay in Section III. Section IV performs the proposed methodology of the algorithm. The results of some fault and overloading cases are discussed in Section V. Finally, Section VII gives a conclusion on this work.

## II. DTLR MATHEMATICAL MODEL

The dynamic rating of the TL is based on the heat-balance equation from IEEE Standard 738 [1]. The steady-state heat balance equation is defined as:

$$I^2R(T_c) = q_c(T_c) + q_r(T_c) - q_s \quad (1)$$

$$I = \sqrt{\frac{q_c(T_c) + q_r(T_c) - q_s}{R(T_c)}} \quad (2)$$

where  $q_c$  is the convection cooling due to air movement,  $q_r$  is the heat removed by radiation,  $q_s$  is solar radiation heat gained from the sun and  $I^2R(T_c)$  is the joule heating gained by current flow in the conductor.  $T_c$  is the conductor temperature.

The convection cooling is given by three different equations  $q_{cn}$ ,  $q_{c1}$  and  $q_{c2}$  for zero wind speed (natural convection), low wind speed and high wind speed, respectively.

$$q_{cn} = 3.645\rho_f^{0.5}D^{0.75}(T_c - T_a)^{1.25} \quad (3)$$

$$q_{c1} = K_{angle} \left[ 1.01 + 1.35 \left( \frac{DV_w\rho_f}{\mu_f} \right)^{0.52} \right] k_f (T_c - T_a) \quad (4)$$

$$q_{c2} = K_{angle} \left[ 0.0119 \left( \frac{DV_w\rho_f}{\mu_f} \right)^{0.6} \right] k_f (T_c - T_a) \quad (5)$$

The convection cooling is chosen based on the largest value of (3), (4) and (5).

$$q_c = \max(q_{cn}, q_{c1}, q_{c2}) \quad (6)$$

where  $\rho_f$  is air density,  $D$  is the conductor outer diameter,  $T_a$  is the ambient temperature,  $K_{angle}$  is the direction factor of wind,  $V_w$  is the wind speed,  $\mu_f$  is the dynamic velocity and  $k_f$  is the thermal conductivity. The formulas of  $\rho_f$ ,  $K_{angle}$ ,  $\mu_f$  and  $k_f$  are given in details in [1].

The heat removed by radiation is calculated as follow:

$$q_r = 0.0178D\varepsilon \left[ \left( \frac{T_c + 273}{100} \right)^4 - \left( \frac{T_a + 273}{100} \right)^4 \right] \quad (7)$$

where  $\varepsilon$  is the emissivity.

The heat gained from the sun is defined as follow:

$$q_s = \alpha Q_{SE} \sin(\theta) A' \quad (8)$$

where  $\alpha$  is the absorptivity of solar,  $Q_{SE}$  is the total solar and sky radiated heat flux corrected for elevation,  $\theta$  is effective angle of incidence of sun rays and  $A'$  is the projected area of conductor per unit length.

**TABLE 1.** Measured impedance based on fault type.

Fault Type	Impedance ( $Z_M$ )
AG	$V_A / (I_A + KI_0)$
BG	$V_B / (I_B + KI_0)$
CG	$V_C / (I_C + KI_0)$
AB-ABG	$(V_A - V_B) / (I_A - I_B)$
BC-BCG	$(V_B - V_C) / (I_B - I_C)$
CA-CAG	$(V_A - V_C) / (I_A - I_C)$
ABC-ABCG	$(V_A / I_A) \text{ OR } (V_B / I_B) \text{ OR } (V_C / I_C)$
	$K = (Z_0 - Z_+) / Z_+ \quad I_0 = (I_A + I_B + I_C) / 3$

where  $V_A$ ,  $V_B$  and  $V_C$  are phase voltages,  $I_A$ ,  $I_B$  and  $I_C$  are phase currents,  $Z_0$  is zero sequence impedance and  $Z_+$  is positive sequence impedance.

The dynamic line rating is calculated based on the real-time measurements of weather conditions and the current. This requires the transient heat balance formula of IEEE Standard 738 to be taken into consideration. The transient formula is defined as:

$$I^2 R(T_c) = q_c(T_c) + q_r(T_c) + mC_p \frac{dT_c}{dt} - q_s \quad (9)$$

$$dT_c = \frac{1}{mC_p} \left[ I^2 R(T_c) - q_c(T_c) - q_r(T_c) + q_s \right] dt \quad (10)$$

where  $mC_p$  is the heat capacity of the conductor.

At each time step, the change in conductor temperature ( $dT_c$ ) is calculated using eq. (10) based on the real-time weather conditions and the actual current in the system. After that, the conductor temperature ( $T_c$ ) is determined based on the change in conductor temperature and the conductor temperature of the previous step. Then, the maximum permissible ampacity can be calculated using eq. (2).

### III. CONVENTIONAL TL PROTECTION

There are many conventional relays used with TL. Distance and overcurrent relays are the most widely conventional relays used in TL protection.

#### A. DISTANCE PROTECTION

Distance relay is based on the measurement of apparent impedance using voltage,  $V$ , and current,  $I$ , phasors at the relay location. The apparent impedance is calculated as follow:

$$Z_M = \frac{V}{I} \quad (11)$$

Depending on the fault type, the measured impedance can vary as illustrated in Table 1 [33]. If the measured impedance is less than the reach point impedance, the relay declares the case as fault and sends a trip signal to the circuit breaker (CB). As the apparent impedance is dependent on the voltage

and current phasors ratio, it may be plotted on an R-X diagram and can be compared with loci of the protected zone impedance. The most popular characteristic that can be used with distance relay is Mho relay. The reach point impedance depends on the zone that the relay protects. The relay has a three forward zones, mainly Zone 1, Zone 2, and Zone 3. It is important to coordinate between the three zones by using time delays. Zone 1 is set as 80 – 85% of the impedance of the protected line to overcome over-reaching problem and it trips instantaneously. Additionally, the setting of Zone 2 is 120 – 150% of the protected line impedance or equal to the protected line impedance plus 50% of the shorted adjacent line [34], [35]. This zone is considered as a back-up protection for Zone 1. So, a time delay of 0.25 – 0.4 s is used with Zone 2 [36]. Zone 3 is called a remote back-up for Zones 1 and 2. Furthermore, the setting of Zone 3 reach point is 220 – 240% of the protected line impedance. The delay setting of Zone 3 is 0.6 – 1 s [34]. In this paper, the zones settings are selected as 80%, 150% and 240% of the protected line impedance for Zone 1, Zone 2 and Zone 3, respectively. In addition, the time delay of Zone 2 and Zone 3 are chosen as 0.4 s and 1 s, respectively.

#### B. OVERCURRENT PROTECTION

The OC relay operates when the measured current is higher than a predetermined pick-up value ( $I_s$ ). The pick-up value of the relay is usually set to 110 – 120% of the nominal current. So, if the operating current exceeds the setting of the relay, it will send a trip signal to CB whether the condition is fault or overload. To use overcurrent protection as back-up protection, the characteristic of the relay used is definite-time. If OC sends a trip signal to CB, it waits for a predefined (delay) time before confirming the case as fault. In the case of definite-time OC relay, a delay of 3 s or less is common with a maximum of 10 s [37]. The delay time is chosen based on the voltage level and is required to be consistent with the standards. For example, based on practical experience, a 1.5 s delay is used with voltage level 66 kV, and 2.5 s is used with 220 kV. Thus, the setting of the relay in this paper is chosen 2 s which is lower than the time that the transmission line can withstand during the maximum short circuit current. Additionally,  $I_s$  is chosen 120% of the nominal current.

### IV. PROPOSED METHODOLOGY

This paper investigates the effect of changing environmental conditions on transmission line DTR, and the effect of faults either symmetrical or asymmetrical, and consequently enhances distance and overcurrent relays performance.

The proposed algorithm consists of three sub-algorithms; DTLR, current ratio of negative and positive sequences and voltage criterion to detect faults and unsafe overloading and restrain the conventional relays during safe overloading. DTLR algorithm detects unsafe overloading and faults whether symmetrical or asymmetrical. If DTLR algorithm fails to detect faults, another criterion is required. As the sym-

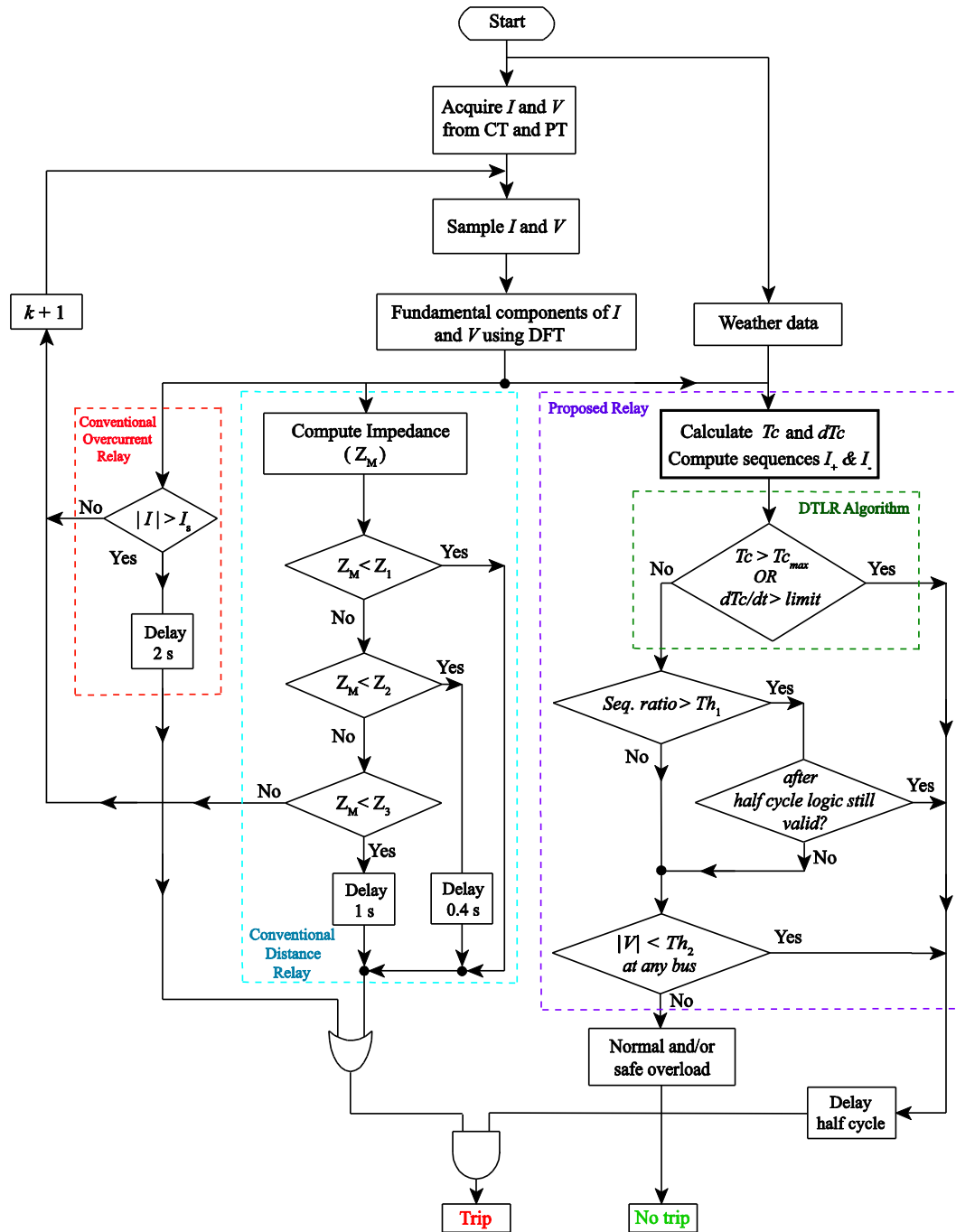


FIGURE 1. Flowchart of the proposed algorithm.

metrical fault and overloading have only positive sequence, the current ratio of negative and positive sequences is used to detect asymmetrical faults. Due to the switching of CB, the negative sequence may have existed for a very limited time. Consequently, a half cycle delay is added to the sequence ratio  $I_-/I_+$  to make sure the case is asymmetrical fault. When this ratio is higher than threshold ( $Th_1$ ) after waiting half cycle, asymmetrical fault is assigned. To differentiate between symmetrical fault and safe overloading, voltage criterion is

used. This criterion uses the fact that the voltage dip during symmetrical fault conditions is high enough compared to overloading conditions. Thus, the 60 Hz component of line voltages is used for this purpose. If the line voltage is lower than predetermined threshold ( $Th_2$ ) value, the relay declares the case as symmetrical fault.

The flowchart of the proposed algorithm is shown in Fig. 1. The first step is acquiring the currents and voltages from the system using current transformer (CT) and potential

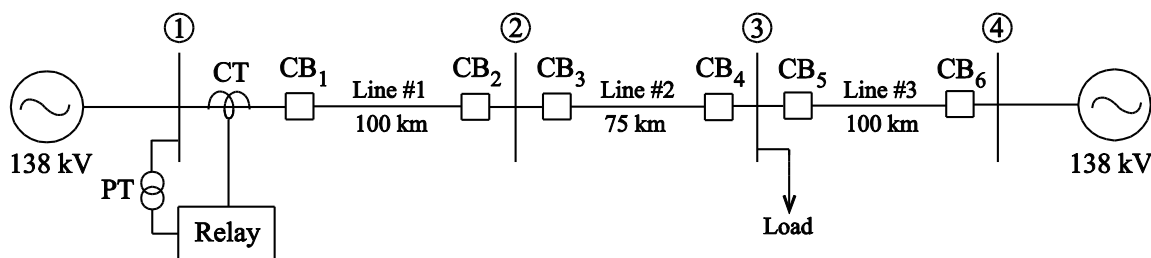


FIGURE 2. System under study.

TABLE 2. Comparison of proposed and conventional relays during overloading and fault conditions.

Case	Switching angle	Time to trip (s)					
		OC Relay	Distance Relay	DTLR alone	Proposed Relay	Final Decision	
<b>Overload Conditions</b>							
Overload with favorable weather conditions	90°	2.008	1.02	No trip	No trip	No trip	
Overload with less favorable weather conditions	90°	2.008	1.02	165.36	165.36	165.36	
<b>Fault Conditions</b>							
Zone #1	AG fault at 50 km of line #1	0°	2.006	0.011	0.016	0.014	0.014
	BC fault at 50 km of line #1	90°	2.006	0.013	0.014	0.013	0.013
	ABCG fault at 70 km of line #1	90°	2.004	0.014	0.013	0.013	0.014
Zone #2	ACG fault at 70 km of line #1	0°	2.006	0.015	0.016	0.016	0.016
	ABC fault at the end of line #1	90°	2.005	0.409	0.014	0.014	0.409
	BG fault at the end of line #1	0°	2.006	0.411	No trip	0.014	0.411
	ABG fault at 40 km of line #2	90°	2.007	0.417	0.021	0.021	0.417
Zone #3	AC fault at 40 km of line #2	0°	2.009	0.419	0.02	0.017	0.419
	BG at the end of line #2	90°	2.012	1.017	No trip	0.02	1.017
	BCG at 20 km of line #3	0°	2.007	1.02	No trip	0.015	1.02
	ABC fault at 20 km of line #3	0°	2.006	1.013	0.02	0.02	1.013
	ABC fault at 50 km of line #3	0°	2.007	1.014	No trip	0.022	1.014
	AB at 50 km of line #3	90°	2.012	1.017	No trip	0.021	1.017

transformer (PT). Then, the fundamental components of currents and voltages are extracted using one cycle discrete Fourier transform (DFT). The algorithm uses three parallel paths: conventional distance relay, conventional OC relay and the proposed algorithm. For distance relay, the measured apparent impedance is calculated using voltage and current. If the impedance is lower than Zone 1 setting ( $Z_1$ ), the relay sends a trip signal instantaneously. Else, if the measured impedance less than Zone 2 reach setting ( $Z_2$ ), a trip signal is sent to CB after a delay of 0.4 s. If the condition is not valid, the relay compares the apparent impedance with Zone 3 setting ( $Z_3$ ). Once the condition of Zone 3 is valid the relay sends a trip signal after 1 s delay. Otherwise, the condition is normal. The logic of OC relay is also checked in parallel with distance relay. If the logic of OC is satisfied, the condition may be fault or overload. The relay waits 2 s before sending a trip signal to CB. This means that if the distance protection failed to detect the fault, the OC relay will trip after its delay

time. Else, a normal condition is confirmed. The decision of both relays (i.e., OC and distance) is enhanced by the decision of the proposed algorithm to increase the dependability and security of the relay.

The first step of the proposed approach is to calculate  $dT_c$  and  $T_c$  at each time step, and the positive and negative sequence currents (i.e.,  $I_+$  and  $I_-$ ). Then, DTLR logic is checked. If the conductor temperature is higher than the maximum conductor temperature ( $T_{c,max}$ ) or the rate of change of conductor temperature violates the *limit*, the relay sends a trip signal. Therefore, the condition is unsafe overload and/or fault either symmetrical or asymmetrical. Else, the condition may be fault and/or overload. Then, the relay checks the sequence ratio. Once the ratio is higher than  $Th_1$  the relay waits a half cycle and checks the ratio again. If the ratio logic is valid, asymmetrical fault is confirmed. Otherwise, the case is symmetrical fault and/or safe overload and/or normal. After that, the voltage criterion is checked.

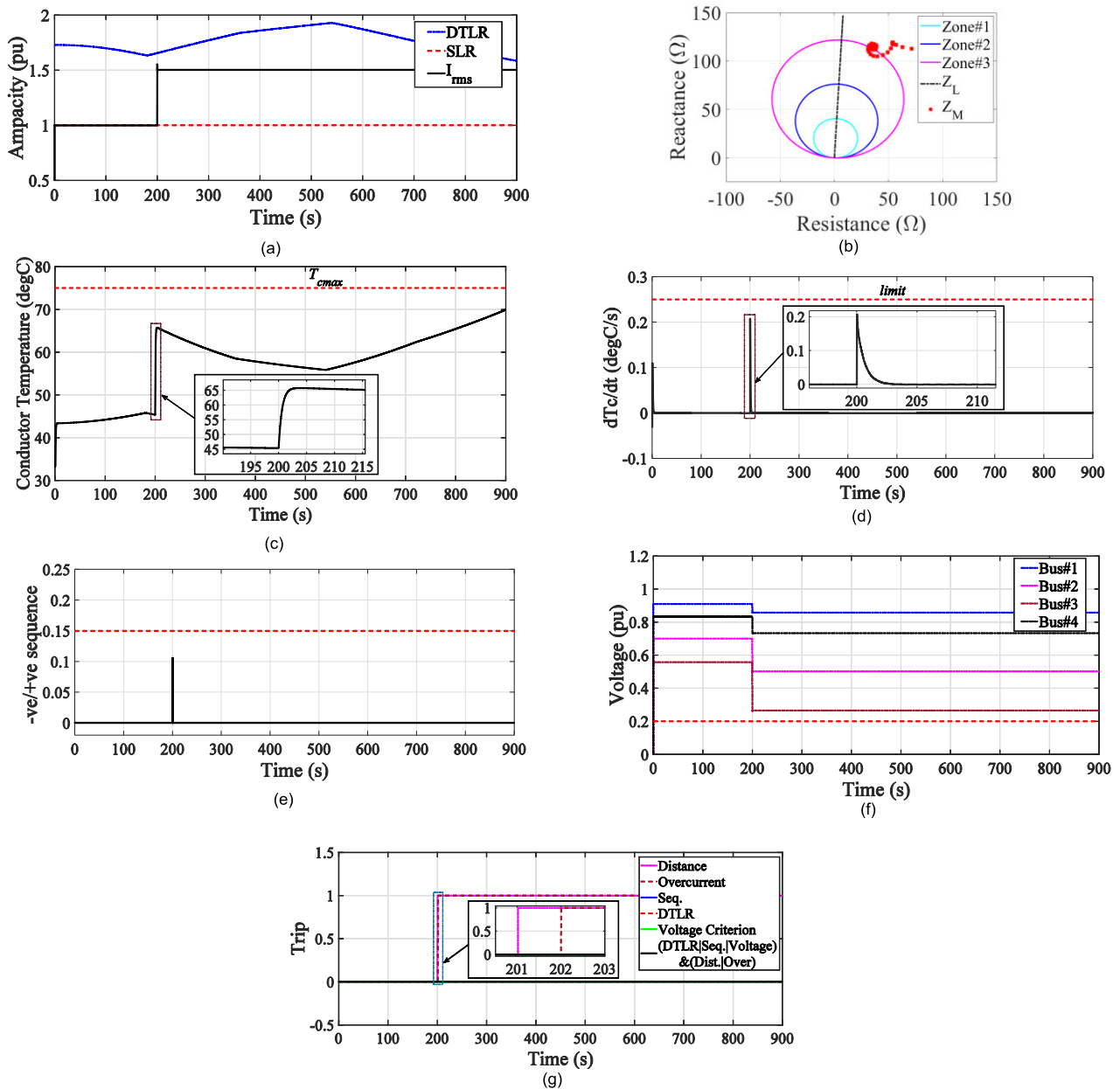


**FIGURE 3.** Relay behaviour during overload case with favorable weather conditions. (a) DTR ampacity and load current, (b) Mho relay characteristic, (c) conductor temperature, (d) conductor temperature rate of change, (e) sequence ratio, (f) voltage criterion, and (g) relays decision.

If the fundamental component of line-to-line voltages at any bus is lower than  $Th_2$  a symmetrical fault is assigned. Else, the case is safe overload and/or normal condition. So, the relay is restrained to send a trip signal. For security purpose of the algorithm, all trip signals sent by the proposed relay is delayed by half cycle to ensure the trip decision is correct.

As symmetrical fault does not have negative sequence component, the current ratio of negative and positive sequences is almost equal to zero. So, the threshold  $Th_1$  is chosen as 0.15 which adds 15% margin above zero. Furthermore, the symmetrical fault is the most severe type, and it is due to short-circuit between the three phases.

So, the bus line voltage might be dropped down close to zero value, unlike overload condition. Consequently, after excessive mathematical analysis of many fault cases  $Th_2$  is chosen 0.2 pu.

### V. SIMULATED SYSTEM

Single line diagram of the transmission system used to assess the proposed algorithm is shown in Fig. 2. It consists of two sources each with a 138 kV rating. The sources are connected to three transmission lines of 100 km, 75 km and 100 km respectively. A load is connected to bus 3. The parameters of the system are given in the appendix.



The system is simulated using MATLAB/Simulink software. The sampling frequency used is 960 Hz. The current transformer connected in each phase has 600/5 turns ratio and the potential transformer is 1200/1.

## VI. RESULTS

The performance of real-time DTLR is investigated on a TL in southern Alberta, Canada. The line with Aluminum Steel Reinforced Conductor (ASRC) 266.8 Partridge has SLR of 537 A, calculated at 75 °C conductor temperature, 0.6 m/s wind speed, 90° of wind direction and ambient temperature of 0 °C. The nominal parameters used to calculate thermal rating are given in the appendix. The weather data is taken from the Environment Canada database at CALGARY INT'L CS station on 16<sup>th</sup> of August 2020 [38]. In this work, it is assumed that the data is updated every 3 minutes. Also, the maximum overloading conditions are 1.5 of nominal current. The maximum conductor temperature used in the analysis of cases is selected as 75 °C. The rate of change of conductor temperature at a load current equal to 1.5 of nominal current has been mathematically calculated and its value is 0.2048 °C/s. So, a *limit* of 0.25 °C/s is chosen in this work. This leaves sufficient margin of almost 18% above overloading limit.

Some case studies describing the results of the proposed scheme are given in detail while the others are summarized in Table 2.

### A. OVERLOADING AT FAVORABLE WEATHER CONDITIONS

A case of overloading with DTLR during favorable weather conditions is shown in Fig. 3. The ampacity is increased between 60% and 90% over SLR as illustrated in Fig. 3a. So, it is assumed that the system operators increased the load at 200 s to 1.5 of nominal current as depicted in Fig. 3a. Consequently, the Mho relay detects this case as fault as seen in the characteristics demonstrated in Fig. 3b. The conductor temperature increased but it is still lower than  $T_{c\max}$  as shown in Fig. 3c. The rate of change in conductor temperature is less than the *limit*, Fig. 3d. Then, the algorithm checks the sequence ratio as depicted in Fig. 3e. It can be seen the ratio has one spike less than  $Th_1$  due to CB switching. After that, the 60 Hz component of line voltage at all buses is checked as seen in Fig. 3f. It can be seen the voltages values are higher than 0.2 indicating that the case is normal operation. The distance and overcurrent relays detected this case as fault, but the combined relay avoids mal-operation of conventional relays and restrained them to trip the CB as observed from Fig. 3g.

### B. OVERLOADING AT LESS FAVORABLE WEATHER CONDITIONS

During less favorable weather conditions, if the load increased the temperature of the conductor may violate the maximum temperature limit. This condition is tested as depicted in Fig. 4. The permissible ampacity is decreased compared to previous case as seen in Fig. 4a. So, the line can

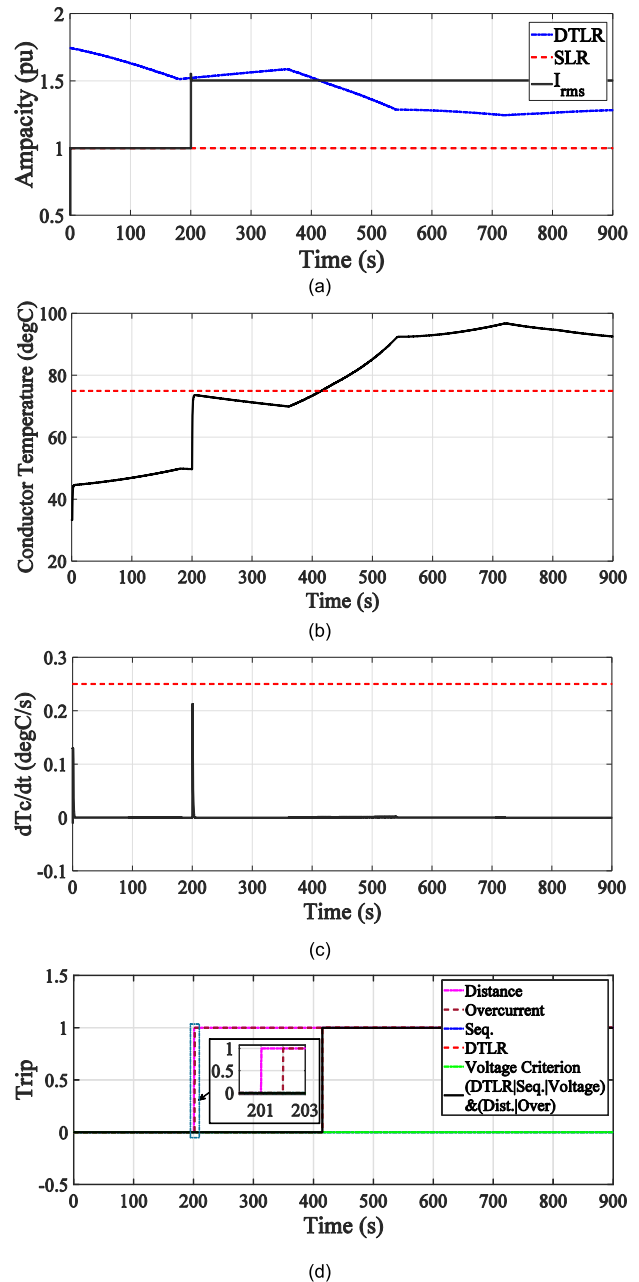


**FIGURE 4.** Relay performance during overload case with less favorable weather conditions. (a) DTR ampacity and load current, (b) conductor temperature, (c) conductor temperature rate of change, and (d) relays decision.

handle the overload for a limited time before the temperature increased over the limit, Fig. 4b. Thus, DTLR algorithm sends a trip signal at 415.36 s as illustrated in Fig. 4d. In this case, system operators may have a choice to decrease the load from 1.5 to 1.2 of nominal current without violating the limits.

### C. THREE-PHASE FAULT AT ZONE 3

To evaluate the algorithm for symmetrical faults, a three-phase to ground fault at 60 km of the third TL has occurred at 200 s, Fig. 5. The rms current is illustrated in Fig. 5a.

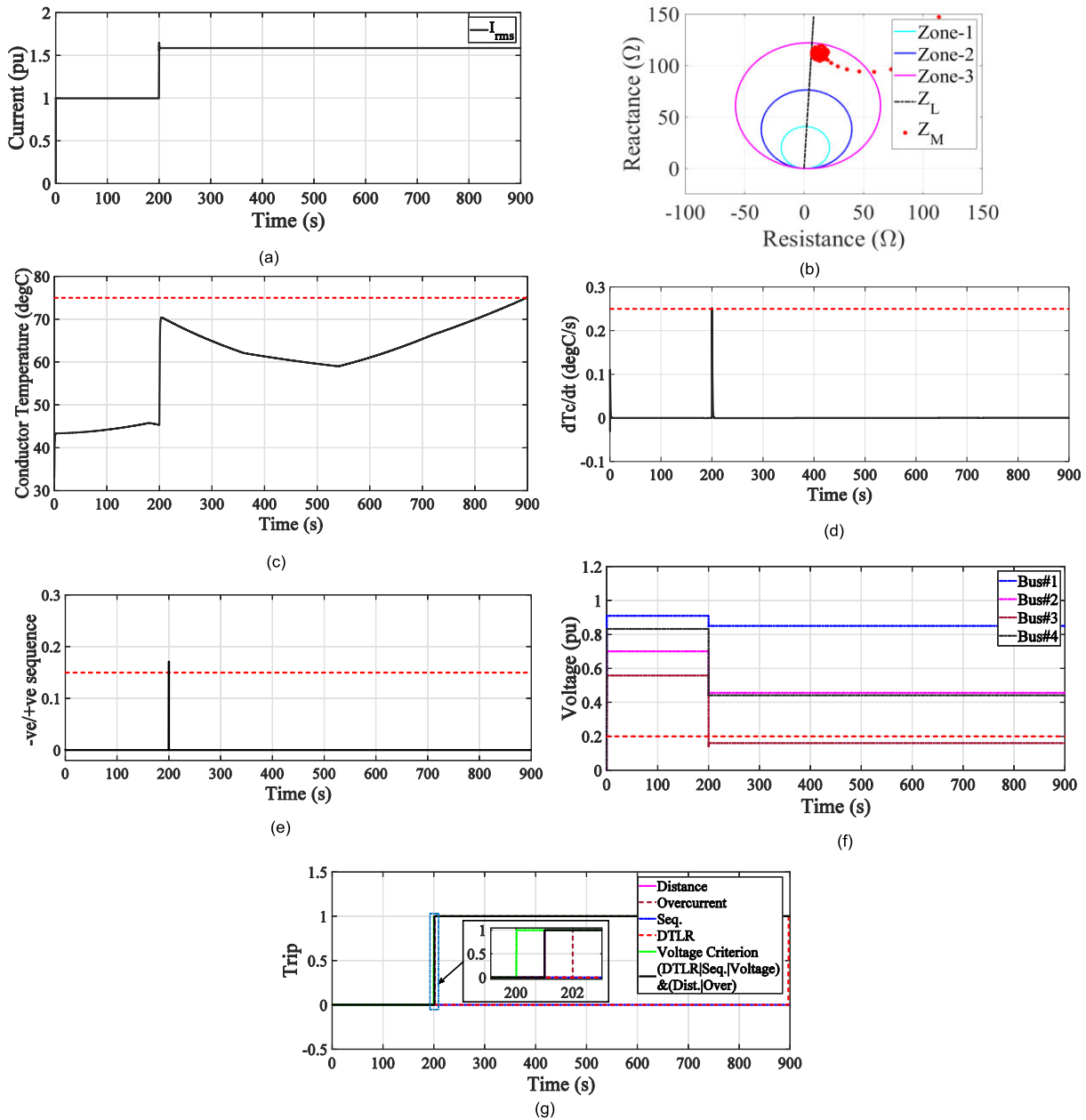


**FIGURE 5.** Relay behaviour during ABCG fault at 60 km of Line #3 (a) fault current, (b) Mho relay characteristic, (c) conductor temperature, (d) conductor temperature rate of change, (e) sequence ratio, (f) voltage criterion, and (g) relays decision.

Additionally, the Mho relay successfully detected the fault as obvious from Fig. 5b. It can be seen from Figs. 5c and 5d the DTLR failed to detect this fault as the conductor temperature and the rate of change in temperature are less than the limits. Then, the algorithm checks the sequence ratio criterion as depicted in Fig. 5e. The ratio has a spike due to CB switching whose duration is less than half cycle and consequently does not give a trip signal, Fig. 5g. In addition, the third bus voltage is lower than 0.2 as seen in Fig. 5f. Thus, the relay sends a trip signal at 201.013 s based on the decision from voltage criterion and distance relay as shown in Fig. 5g.

**D. SLG FAULT AT ZONE 3**

A phase ‘C’ to ground fault takes place on 20 km of the third line at 200 s as seen in Fig. 6. Mho relay detects the fault in Zone 3 as depicted in Fig. 6b. Moreover, the conductor temperature is lower than its maximum limit as illustrated when the conductor temperature is less than the *limit*, Fig. 6d. This means that the DTLR criterion failed to detect this fault. Consequently, the algorithm checked the sequence ratio and confirmed that the ratio is higher than 0.15 as shown in Fig. 6e. Therefore, the relay sent a trip signal at 201.019 s based on the action from Mho and sequence ratio criterion as demonstrated in Fig. 6f.



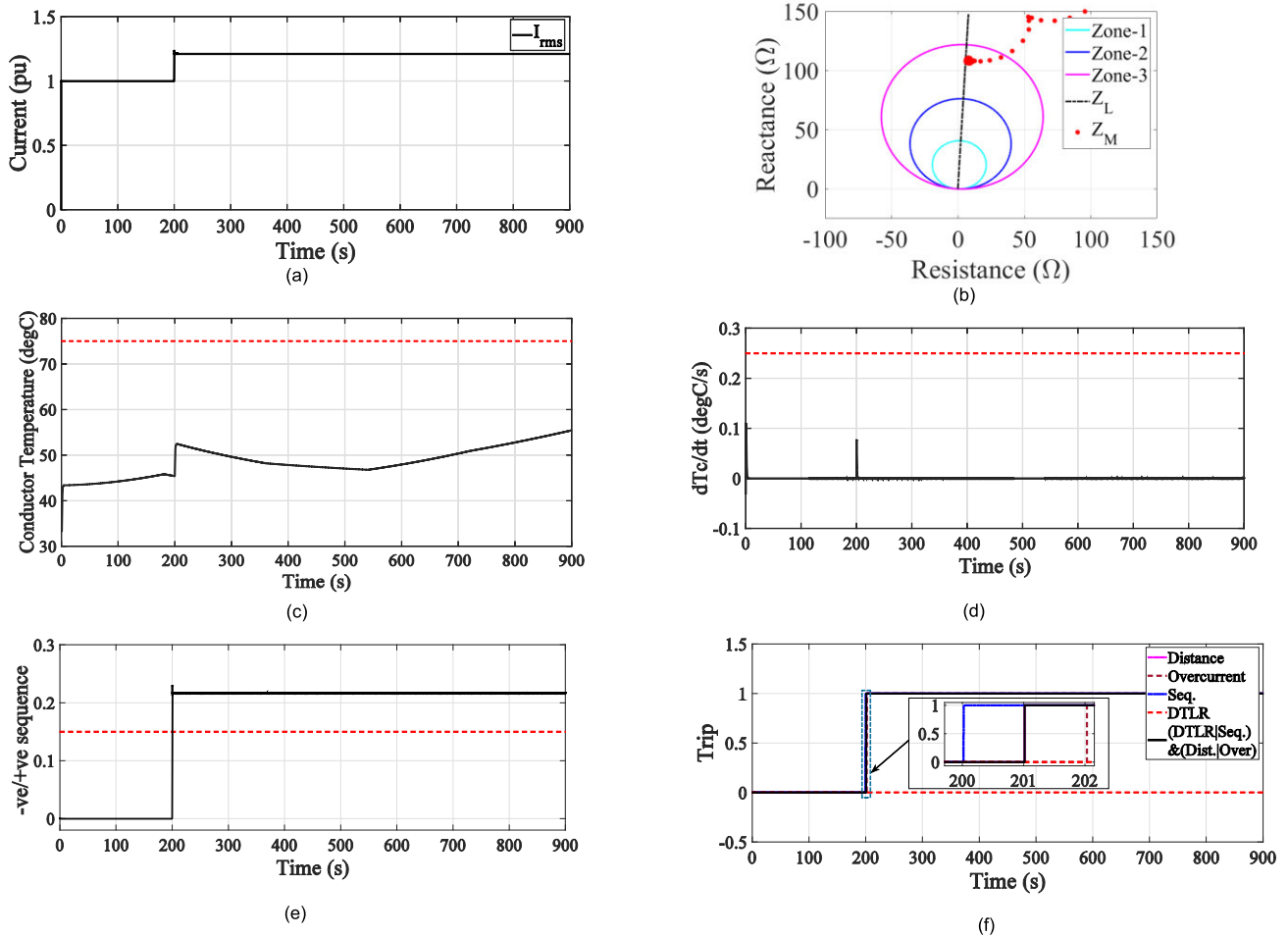


**FIGURE 6.** Relay performance during CG fault at 20 km of Line #3 (a) fault current, (b) Mho relay characteristic, (c) conductor temperature, (d) conductor temperature rate of change, (e) sequence ratio, and (f) relays decision.

**E. OTHER STUDIES**

To evaluate the performance of the proposed algorithm, many fault cases and some of overloading have been investigated at different switching angle, 0° (i.e., 250 s) and 90° (i.e., 250.004166 s) of phase ‘A’ voltage. The results are summarized in Table 2. It can be seen from Table 2 that the conventional relays mal-operated and sent a trip signal during overloading cases whether the weather conditions were favorable or less favorable. In addition, the proposed algorithm successfully detected the overload as a fault condition after the conductor temperature violated the limit with less favorable weather conditions. This means that the system operators can use the full benefits from the TL unless the thresholds and limits that used in the proposed algorithm are not violated. During fault conditions, if DTLR algorithm is used alone, it may not detect the fault conditions that are far from the relay location, namely Zone 2 or Zone 3. Unlike using DTLR algorithm alone, the proposed algorithm successfully detected all types of faults within one and quarter cycle after the standard delays used.

**VII. CONCLUSION**

The increase integration of renewable generation to power grids leads to utilizing of dynamic thermal rating to satisfy these generation without changing the infrastructure of existing transmission lines. Consequently, increasing of load affects the performance of existing conventional relays and it is difficult to differentiate between fault and overload conditions. To the best of our knowledge, this work is the first proposal of an enhanced algorithm augmented with conventional relays in the presence of DTLR to detect all fault conditions whether they are symmetrical or asymmetrical and unsafe overload, and restrain the CB during safe overload. The proposed algorithm is based on three sub-algorithms: DTLR, current ratio of negative and positive sequences, and voltage criterion. DTLR is used to detect unsafe overloading and all types of faults either symmetrical or asymmetrical. Furthermore, asymmetrical faults have been detected using the current ratio of sequences. In addition, the voltage criterion is used to discriminate symmetrical faults from safe overloading.

Many overloading and fault cases have been investigated in this paper. The results at hand show that the proposed scheme can successfully differentiate between faults, unsafe and safe overloading. All fault conditions are detected within cycle and quarter plus the delays used in the settings. It is evidenced that the proposed algorithm is reliable and efficient in detecting the faults and restraining the CB during safe overloading resulting from dynamic thermal rating. The algorithm is simple to implement and is proposed to be tested on a physical transmission line as the next step.

## APPENDIX

**TABLE 3. Simulated power system parameters.**

	Parameter	Value/Units
Sources	Nominal Voltage	138 kV
	Frequency	60 Hz
	Source strength	1000, 750 MVA
	X/R	3.5, 5
Transmission Line	Positive sequence impedance ( $Z_+$ )	$0.0275 + j0.507053 \Omega/\text{km}$
	Zero sequence impedance ( $Z_0$ )	$0.275 + j1.4043 \Omega/\text{km}$
	Positive sequence capacitance	9.483 nf/km
	Zero sequence capacitance	6.711 nf/km
Load (inductive)	Power	335 MW
	Power factor	0.8

**TABLE 4. Nominal parameters used to calculate thermal rating.**

Parameter	Symbol	Value/Units
Maximum conductor temperature	$T_{cmax}$	75 °C
Diameter	$D$	16.3 mm
Elevation above sea level	$H_e$	1030 m
Emissivity	$\epsilon$	0.6
Solar absorption coefficient	$\alpha_s$	0.8
Latitude	Lat	50°
Solar declination	$\delta$	23.45°
Hour angle	$\omega$	0°
Line azimuth	$Z_l$	0°

## ACKNOWLEDGMENT

The lead author wishes to thank Leanne Dawson for her help.

## REFERENCES

- [1] IEEE Standard for Calculating the Current-Temperature Relationship of Bare Overhead Conductors, Standard 738-2012 Revision of IEEE Std 738-2006 Std 738-2012 Cor 1-2013, 2013, pp. 1–72, doi: 10.1109/IEEESTD.2013.6692858.
- [2] R. Dupin and A. Michiorri, “Dynamic line rating forecasting,” in *Renewable Energy Forecasting: From Models to Applications* Amsterdam, The Netherlands: Elsevier, 2017, pp. 325–339, doi: 10.1016/B978-0-08-100504-0.00013-5.
- [3] L. Dawson and A. M. Knight, “Applicability of dynamic thermal line rating for long lines,” *IEEE Trans. Power Del.*, vol. 33, no. 2, pp. 719–727, Apr. 2018, doi: 10.1109/TPWRD.2017.2691671.
- [4] *Oncor’s Pioneering Transmission Dynamic Line Rating (DLR) Demonstration Lays Foundation for Follow-on Deployments*, U.S. Dept. Energy, Baltimore, MD, USA, 2014.
- [5] W. Jiang, J. Lu, H. Xiang, X. Ma, and H. Fang, “Distance protection of EHV long transmission lines considering compensation degree of shunt reactor,” *Global Energy Interconnection*, vol. 2, no. 1, pp. 64–70, Feb. 2019, doi: 10.1016/j.gloi.2019.06.008.
- [6] M. Nojavan, H. Seyedi, and M. Mehdinejad, “A novel scheme for current-only directional overcurrent relay,” *Int. J. Electr. Power Energy Syst.*, vol. 82, pp. 252–263, Nov. 2016, doi: 10.1016/j.ijepes.2016.03.021.
- [7] M. Singh, B. K. Panigrahi, and A. R. Abhyankar, “Combined optimal distance to overcurrent relay coordination,” in *Proc. IEEE Int. Conf. Power Electron., Drives Energy Syst. (PEDES)*, Dec. 2012, pp. 1–6, doi: 10.1109/PEDES.2012.6484300.
- [8] H. Weng, H. Chen, L. Wu, J. Huang, and Z. Li, “A novel pilot protection scheme for transmission lines based on current distribution histograms and their Bhattacharyya coefficient,” *Electr. Power Syst. Res.*, vol. 194, May 2021, Art. no. 107056, doi: 10.1016/j.epsr.2021.107056.
- [9] A. Ghorbani, H. Mehrjerdi, H. Heydari, and S. Ghanimati, “A pilot protection algorithm for TCSC compensated transmission line with accurate fault location capability,” *Int. J. Electr. Power Energy Syst.*, vol. 122, Nov. 2020, Art. no. 106191, doi: 10.1016/j.ijepes.2020.106191.
- [10] M. Farshad, “A pilot protection scheme for transmission lines of half-bridge MMC-HVDC grids using cosine distance criterion,” *IEEE Trans. Power Del.*, vol. 36, no. 2, pp. 1089–1096, Apr. 2021, doi: 10.1109/TPWRD.2020.3001878.
- [11] S. Unde and S. Dambhare, “Current differential protection of double-circuit transmission lines in modal domain,” *Electr. Eng.*, vol. 102, no. 4, pp. 2401–2411, Dec. 2020, doi: 10.1007/s00202-020-01038-y.
- [12] S. M. Hashemi and M. Sanaye-Pasand, “Current-based out-of-step detection method to enhance line differential protection,” *IEEE Trans. Power Del.*, vol. 34, no. 2, pp. 448–456, Apr. 2019, doi: 10.1109/TPWRD.2018.2873698.
- [13] R. L. D. S. Franca, F. C. D. S. Junior, T. R. Honorato, J. P. G. Ribeiro, F. B. Costa, F. V. Lopes, and K. S. Strunz, “Traveling wave-based transmission line earth fault distance protection,” *IEEE Trans. Power Del.*, vol. 36, no. 2, pp. 544–553, Apr. 2021, doi: 10.1109/TPWRD.2020.2984585.
- [14] M. Khalili, F. Namdari, and E. Rokrok, “Traveling wave-based protection for SVC connected transmission lines using game theory,” *Int. J. Electr. Power Energy Syst.*, vol. 123, Dec. 2020, Art. no. 106276, doi: 10.1016/j.ijepes.2020.106276.
- [15] F. V. Lopes, K. M. Dantas, K. M. Silva, and F. B. Costa, “Accurate two-terminal transmission line fault location using traveling waves,” *IEEE Trans. Power Del.*, vol. 33, no. 2, pp. 873–880, Apr. 2018, doi: 10.1109/TPWRD.2017.2711262.
- [16] H. A. Jimenez, D. Guillen, R. Tapia-Olvera, G. Escobar, and F. Beltran-Carbajal, “An improved algorithm for fault detection and location in multi-terminal transmission lines based on wavelet correlation modes,” *Electr. Power Syst. Res.*, vol. 192, Mar. 2021, Art. no. 106953, doi: 10.1016/j.epsr.2020.106953.
- [17] A. R. Adly, S. H. E. A. Aleem, M. A. Algabalawy, F. Jurado, and Z. M. Ali, “A novel protection scheme for multi-terminal transmission lines based on wavelet transform,” *Electr. Power Syst. Res.*, vol. 183, Jun. 2020, Art. no. 106286, doi: 10.1016/j.epsr.2020.106286.
- [18] B. Rathore and A. G. Shaik, “Wavelet-alienation based transmission line protection scheme,” *IET Gener., Transmiss. Distrib.*, vol. 11, no. 4, pp. 995–1003, Mar. 2017, doi: 10.1049/iet-gtd.2016.1022.
- [19] B. Chatterjee and S. Debnath, “A new protection scheme for transmission lines utilizing positive sequence fault components,” *Electr. Power Syst. Res.*, vol. 190, Jan. 2021, Art. no. 106847, doi: 10.1016/j.epsr.2020.106847.
- [20] O. A. Gashteroodkhani, M. Majidi, and M. Etezadi-Amoli, “A fault data based method for zero-sequence impedance estimation of mutually coupled transmission lines,” *IEEE Trans. Power Del.*, vol. 36, no. 5, pp. 2768–2776, Oct. 2021, doi: 10.1109/TPWRD.2020.3026672.

- [21] A. Ghorbani and H. Mehrjerdi, "Negative-sequence network based fault location scheme for double-circuit multi-terminal transmission lines," *IEEE Trans. Power Del.*, vol. 34, no. 3, pp. 1109–1117, Jun. 2019, doi: [10.1109/TPWRD.2019.2906056](https://doi.org/10.1109/TPWRD.2019.2906056).
- [22] L. Ji, X. Tao, Y. Fu, Y. Fu, Y. Mi, and Z. Li, "A new single ended fault location method for transmission line based on positive sequence superimposed network during auto-reclosing," *IEEE Trans. Power Del.*, vol. 34, no. 3, pp. 1019–1029, 2019, doi: [10.1109/TPWRD.2019.2901835](https://doi.org/10.1109/TPWRD.2019.2901835).
- [23] J. S. A. Carneiro and L. Ferrarini, "A probabilistic protection against thermal overloads of transmission lines," *Electr. Power Syst. Res.*, vol. 81, no. 10, pp. 1874–1880, Oct. 2011, doi: [10.1016/j.epsr.2011.05.011](https://doi.org/10.1016/j.epsr.2011.05.011).
- [24] J. S. A. Carneiro and L. Ferrarini, "Analysis and design of overload protections for HV lines with a probabilistic approach," in *Proc. 10th Int. Conf. Probabilistic Methods Appl. Power Syst. (PMAPS)*, 2008, pp. 1–6.
- [25] T. Yip, C. An, G. Lloyd, M. Aten, and B. Ferris, "Dynamic line rating protection for wind farm connections," in *Proc. Symp. Integr. Wide-Scale Renew. Resour. Power Deliv. Syst.*, 2009, pp. 1–5.
- [26] G. Lloyd, G. Millar, T. Yip, and C. An, "Design and field experience of a dynamic line rating protection," in *Proc. Int. Conf. Adv. Power Syst. Autom. Protection*, Oct. 2011, pp. 1068–1073, doi: [10.1109/APAP.2011.6180707](https://doi.org/10.1109/APAP.2011.6180707).
- [27] H. T. Yip, C. An, G. J. Lloyd, M. Aten, R. Ferris, and G. Hagan, "Field experiences with dynamic line rating protection," in *Proc. 10th IET Int. Conf. Develop. Power Syst. Protection (DPSP)*, 2010, pp. 1–5, doi: [10.1049/cp.2010.0219](https://doi.org/10.1049/cp.2010.0219).
- [28] Y. Cong, P. Regulski, P. Wall, M. Osborne, and V. Terzija, "On the use of dynamic thermal-line ratings for improving operational tripping schemes," *IEEE Trans. Power Del.*, vol. 31, no. 4, pp. 1891–1900, Aug. 2016, doi: [10.1109/TPWRD.2015.2502999](https://doi.org/10.1109/TPWRD.2015.2502999).
- [29] M. K. Metwaly and J. Teh, "Fuzzy dynamic thermal rating system-based SIPS for enhancing transmission line security," *IEEE Access*, vol. 9, pp. 83628–83641, 2021, doi: [10.1109/ACCESS.2021.3086866](https://doi.org/10.1109/ACCESS.2021.3086866).
- [30] Ā. Staszewski and W. Rebizant, "DLR-supported overcurrent line protection for blackout prevention," *Electr. Power Syst. Res.*, vol. 155, pp. 104–110, Feb. 2018, doi: [10.1016/j.epsr.2017.10.009](https://doi.org/10.1016/j.epsr.2017.10.009).
- [31] L. Staszewski and W. Rebizant, "DLR-supported distance protection for blackout mitigation," in *Proc. 2016 Electr. Power Netw. (EPNet)*, 2016, pp. 1–6, doi: [10.1109/EPNET.2016.7999359](https://doi.org/10.1109/EPNET.2016.7999359).
- [32] IEEE Power System Relaying Committee Working Group, "Single phase tripping and auto reclosing of transmission lines—IEEE Committee Report," *IEEE Trans. Power Del.*, vol. 7, no. 1, pp. 182–192, 1992, doi: [10.1109/61.108906](https://doi.org/10.1109/61.108906).
- [33] *IEEE Guide for Protective Relay Applications to Transmission Lines*, Standard C37.113-2015 Std C37.113-1999, 2016, pp. 1–141, doi: [10.1109/IEEESTD.2016.7502047](https://doi.org/10.1109/IEEESTD.2016.7502047).
- [34] J. M. Gers and E. J. Holmes, *Protection of Electricity Distribution Networks*. London, U.K.: IET, 2011.
- [35] P. M. Anderson, *Power system Protection*. Hoboken, NJ, USA: Wiley, 1999.
- [36] J. D. J. Jaramillo Serna and J. M. López-Lezama, "Calculation of distance protection settings in mutually coupled transmission lines: A comparative analysis," *Energies*, vol. 12, no. 7, p. 1290, Apr. 2019, doi: [10.3390/en12071290](https://doi.org/10.3390/en12071290).
- [37] M. Bamber *et al.*, *Network Protection & Automation Guide*. Paris, France: Alstom Grid, May 2011.
- [38] Environment Canada. (2020) *Historical Climate Data*. [Online]. Available: <http://climate.weather.gc.ca/>



dynamic thermal line rating.

**ELSAED ALI** (Member, IEEE) received the B.Sc. and M.Sc. degrees in electrical engineering from Mansoura University, Mansoura, Egypt, in 2007 and 2011, respectively, and the Ph.D. degree in electrical engineering from the University of Calgary, Calgary, Canada, in 2020.

His research interests include power system analysis, power system protection, integration of renewable energy resources in electrical power systems, smart grids operation, power quality, and



**ANDREW M. KNIGHT** (Senior Member, IEEE) received the B.A. and Ph.D. degrees from the University of Cambridge, in 1994 and 1998, respectively.

He is a Professor and the Head of the Department of Electrical and Software Engineering, University of Calgary. His research interests include energy conversion and clean and efficient energy utilization. He is a Professional Engineer registered in the Province of Alberta, Canada. He is a recipient of the IEEE PES Prize Paper Award and three Best Paper Awards from IEEE IAS. He is currently the Vice President of IEEE IAS and was previously the IAS Publications Chair, the Steering Committee Chair of IEEE ECCE and IEEE IEMDC, and the Chair of IEEE Smart Grid Research and Development Committee.

• • •